PROPERTIES OF A PURIFIED PORE-FORMING PROTEIN (PERFORIN 1) ISOLATED FROM H-2-RESTRICTED CYTOTOXIC T CELL GRANULES

By JOHN DING-E YOUNG, ECKHARD R. PODACK,* AND ZANVIL A. COHN

*From The Rockefeller University, New York 10021; and the *Department of Microbiology and Immunology, New York Medical College, Valhalla, New York 10595*

Cytotoxic T lymphocytes and NK cells lyse target cells by a contact-dependent mechanism (reviewed in references 1–4). On target membranes, the lesions formed by these effector cells have been identified as circular rings, resembling complement-induced transmembrane tubules (5–7). The cytolytic function of these cells has been localized to the granule population (8–13). Granules isolated from cytotoxic T lymphocytes produce circular lesions on target membranes (8–13), depolarize the membrane potential of nucleated cells (13), induce marker release from lipid vesicles (11), and induce the formation of large, aqueous channels in planar lipid bilayers (12, 13). A hemolytic pore-forming protein (PFP,[1] also named perforin 1 or P1) of 66 kD (14) and 70–75 kD (15) from the granules of H-2-restricted cytotoxic T cells has recently been isolated. Here, studies on its mechanism of action and its functional properties, using cells and model lipid bilayers as target membranes, are reported. We show that the purified protein polymerizes in the presence of calcium and that it lyses tumor cells, bypassing the requirement for intact cells and granules. Single channels and other electrical characteristics associated with the purified protein were also resolved using high-impedance planar bilayers.

Materials and Methods

Cell Cultures and Isolation of Granules. The mouse cytotoxic T cell lines CTLL-A2, CTLL-A11, and CTLL-R8 were propagated in IL-2-containing medium, as described previously (13, 16). CTLL-A2 and CTLL-A11 specifically lyse target cells expressing $H2D^d$, whereas CTLL-R8 react to a unique determinant on RL♂1 cells. After growing to confluence in large Petri dishes, cells were detached with PBS containing 0.05% EDTA. For preparation of granules, $5–20 \times 10^8$ cells were disrupted by N_2 cavitation (400 pounds per square inch for 25 min) and the nucleus-free supernatant was subjected to Percoll gradient centrifugation, as described (13, 17). Granule enrichment was assessed by hemolytic and β-glucuronidase activities (13, 18). Granules were pelleted and separated

Supported in part by grants from the Cancer Research Institute and Lucille P. Markey Charitable Trust to J. Young during different parts of this research; grants CA-30198 and AI-070127 from National Institutes of Health to Z. Cohn; and U. S. Public Health Service grants CA-39201 and AI-21999, and American Cancer Society grant IM396 to E. Podack. J. Young is a Lucille P. Markey Scholar.

[1] *Abbreviations used in this paper:* PFP/P1 pore-forming protein/perforin 1; TBS, tris-buffered saline.

from Percoll by centrifugation at 180,000 *g* for 2 h at 4°C, using a SW41 rotor (Beckman Instruments, Inc., Fullerton, CA).

Isolation of PFP/P1 from Granules. PFP/P1 was extracted from granules of CTLL-A2, A11, and R8 after two protocols developed simultaneously in our laboratories, yielding similar results. In method I, granules were extracted with 0.2 ammonium acetate, pH 5, containing 1 mM PMSF and 3 mM NaN_3 for 30 min on ice. The granule suspension was then centrifuged at 100,000 *g* for 90 min at 4°C. The clear supernatant was eluted through a Sephadex G-75 column (2.5 cm × 70 cm), equilibrated with 0.1 M ammonium acetate buffer, pH 5, containing 3 mM NaN_3, 1 mM EDTA, and 10% glycerol. Material that was hemolytically active and that formed pores in planar bilayers was pooled, applied to an AG 50 (Bio-Rad Laboratories, Richmond, CA), and eluted with a linear gradient of 0–1 M ammonium acetate, pH 7, 1 mM EDTA, and 10% glycerol. The hemolytically active fractions were collected and applied to a TSK-G3000 SW column (LKB-Produkter AB, Bromma, Sweden), and eluted with 0.1 M sodium phosphate buffer, pH 7, containing 1 mM EDTA, at a flow rate of 0.12 ml/min.

In method II, granules were extracted with 1 M $NaKHPO_4$ buffer containing 1 mM EDTA, 10 mM benzamidine, and 1 mM PMSF, followed by sieving through Sephacryl-S300 column and ion-exchange through Mono Q column (Pharmacia Fine Chemicals, Uppsala, Sweden), essentially as described previously (15, 18). The purified protein was used directly in functional assays or further purified through a TSK G3000 column, as described above. The PFP/P1 purified by these two protocols gave similar results in the functional assays.

Hemolysis Assay. A hemolysis microassay was performed in 96-well plates using a Microplate Reader (Model EL307, Bio-Tek Instruments, Inc., Burlington, VT), as described previously (19). Lysis of SRBC was monitored by A_{690}, which gives a turbidity reading of the cell suspension. This assay allowed rapid screening of membrane lytic activity in fractions obtained from each chromatography column. For evaluation of the hemolytic activity as a function of PFP/P1 concentration, the hemolysis assay was performed in parallel with the ^{51}Cr release from nucleated cells. The total vol per assay was 100 μl, with SRBC at a 20% hematocrit in tris-buffered saline (TBS; 10 mM Tris-HCl, 0.15 M NaCl, pH 7.4) containing 5 mM $CaCl_2$, and the final hemolytic activity after 30 min incubation with PFP/P1 at 37°C was assayed as described (9).

Cytolysis Assay Using ^{51}Cr Release. Lysis of the murine T lymphoma cell line E14 was assayed by ^{51}Cr release, as described (9). Cells were grown in serum-free medium (Iscove's medium), labeled with ^{51}Cr, washed three times in HBSS, and resuspended to 2×10^4 cells per 100 μl per assay. Following addition of PFP/P1 to the indicated concentrations, $CaCl_2$ was immediately added to a final concentration of 5 mM to initiate lysis reaction. ^{51}Cr release was assayed following incubation for 30 min at 37°C, in triplicates.

Formation of Lipid Vesicles. Lipid vesicles were prepared by a one-step detergent-dilution procedure (20). A mixture of 50 mg/ml soybean phospholipids (lecithin, type II, Sigma Chemical Co., St. Louis, MO), previously extracted with acetone (21) and 25 mM β-D-octylglucoside (Calbiochem-Behring, La Jolla, CA) in a 10 mM Hepes buffer, pH 7 (adjusted with Tris-base), containing 0.1 M NaCl, 5 mM $CaCl_2$, and 3 mM NaN_3 (buffer A), was sonicated to clarity. Vesicles were then formed by a one-step 1:100 dilution in the same buffer A, without detergent. Lipid vesicles with diameter of 100–400 nm (as observed by negative contrast electron micrsocopy, not shown) were formed by this simple procedure. The lipid vesicles were sedimented at 100,000 *g* for 90 min and resuspended in buffer A before use.

Incorporation of PFP/P1 into Lipid Vesicles. 2 μg of PFP/P1 was incubated with 5 mg of lipid vesicles in buffer A at 37°C for 48 h. PFP/P1-proteoliposomes were then washed and separated from soluble protein by two centrifugations at 100,000 *g* for 90 min, and resuspended in 50 μl of same buffer. This vesicle preparation was used for fusion with planar bilayers.

To visualize the reconstituted protein by gel electrophoresis, PFP/P1 was incubated with egg lecithin vesicles (type VI; Sigma Chemical Co.) formed by probe-sonication at a ratio of 2 μg protein:2 mg lipid in 0.1 M sodium phosphate buffer, pH 7, containing 5

mM $CaCl_2$, for 48 h at 37°C. Proteoliposomes were sedimented by high-speed centrifugation (100,000 *g*, 90 min, 4°C) and extracted with diethyl ether (three times before applying to a gel slab. To test the effect of Ca^{2+} on polymerization, PFP/P1 was also incubated with lipid vesicles in phosphate buffer in the absence of Ca^{2+} and similarly extracted before gel electrophoresis (Fig. 1, lane *3*).

Planar Bilayer Measurements. Planar bilayers were formed in indicated buffers according to previously published protocols (22, 23). Bilayer membranes were formed from monolayers of soybean phospholipids (Montal and Mueller's technique [24]). Positive current was taken as that flowing from *cis* to *trans* side, with *trans* side defined as the virtual ground. The bilayer conductance was expressed in siemens. The baseline conductance was 5–10 pS and capacitance ranged from 0.71 to 0.73 $\mu F/cm^2$. PFP/P1 was always added to the *cis* side, followed by vigorous stirring for 10–25 s by small rotating magnetic bars.

Fusion of Proteoliposomes with Planar Bilayers. Fusion of vesicles with planar bilayers was implemented by osmotic stress (25, 26). The bilayers were formed in buffer A. The phospholipid used to form the monolayers was suspended in decane/hexane (50:50). 50 μl of proteoliposomes prepared as described above were added to the *cis* side, followed by addition of 300 mM urea to the same side. The bilayer was perfused with 10 vol of urea-free buffer A before channel recording.

Microelectrode Impalement of Nucleated Cells. Chicken embryo myocytes were derived from primary cultures (18, 27) and impaled by standard electrophysiological techniques (28). Cells were dissected from thigh and breast muscles and plated at 5×10^5/ml on collagen-coated dishes and cultured in DME supplemented with 3% FCS and 3% chicken embryo extract (Gibco Laboratories, Grand Island, NY). Arabinoside C (Sigma Chemical Co.) was added on day 3 to 10^{-5} M for 48 h. Cells on days 6–9 were washed in low-K^+ buffer (118 mM NaCl, 5 mM KCl, 1.3 mM $CaCl_2$, 0.8 mM $MgSO_4$, 5.5 mM glucose, 20 mM Hepes, 9 mM Na_2CO_3, pH 7.4) and impaled with microelectrodes filled with 3 M KCl and having resistance ranging from 40 to 90 MΩ. The membrane potential was allowed to stabilize for 10–15 min before application of PFP/P1. 1 μg PFP/P1 was added within 100 μm of the cell by means of a micropipette. The decrease of membrane resistance was evaluated by the application of current pulses of 0.6 nA.

Electron Microscopy. 10^9 SRBC were incubated with PFP/P1 (at concentrations resulting in 10 times 100% hemolysis) for 1 h at 37°C in TBS containing 5 mM $CaCl_2$. Erythrocyte ghosts were collected by centrifugation in 5 mM EDTA, pH 7.4. The final pellet was resuspended in TBS and digested with 100 μg/ml trypsin for 16 h at room temperature. After two more washes in TBS, the membranes were mounted on grids and negatively stained with 2% uranyl formate.

Gel Electrophoresis. Gel slabs were performed according to Laemmli (29), using 4–11% gradient polyacrylamide (20 cm long). An additional 3 cm of 4% gel was added over running gel to resolve high M_r bands. Gels were stained with Coomassie Blue, destained, and restained with silver nitrate (using a kit from Bio-Rad Laboratories). The PFP/P1 used for SDS-PAGE was obtained by method I, outlined above. Samples were boiled in Neville's buffer containing 50 mM DTT for 3 min.

Results

Polymerization of PFP/P1 in the Presence of Ca^{2+}. The granules isolated from the H-2-specific cytotoxic T cell lines show potent hemolytic activity only in the presence of Ca^{2+} (13), and when applied to cells they induced immediate membrane depolarization (13). Granules extracted with ammonium acetate or phosphate released soluble proteins that could assemble into macromolecular ring-like structures after incubation at 37°C (13). The monomeric protein responsible for pore-formation and hemolysis was purified by a combination of molecular sieving and ion-exchange chromatography and migrated on SDS-PAGE slabs as a 70–75 kD protein (Fig. 1, lane *1*). This protein polymerized

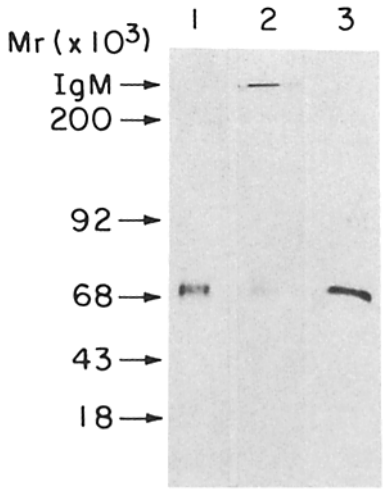

FIGURE 1. SDS-polyacrylamide gel profile of isolated PFP/P1 and Ca^{2+}–dependent polymerization. Lane *1*: 2 μg PFP/P1 isolated from CTLL-All. Lane *2*: 5 μg PFP/P1 reconstituted into lipid vesicles and extracted with diethyl ether (see Materials and Methods). Note that most of the sample migrated very little, remaining on top of the gel. The position of the IgM marker (900,000) is shown for comparison. Lane *3*: 5 μg PFP/P1 incubated with lipid vesicles, as in lane *2*, however, in the absence of Ca^{2+}.

spontaneously at 37°C only in the presence of Ca^{2+} (Fig. 1, lane *2*). In Ca^{2+}-free conditions, polymerization was not observed (Fig. 1, lane *3*). The polymer formed this way became at least partially resistant to dissociation by SDS and reducing agents, as evidenced by the fact that it remained as a polymeric species of $M_r > 10^6$ daltons during gel electrophoresis (Fig. 1, *lane 2*).

Ultrastructural examination of this isolated protein incubated at 37°C showed tubular complexes similar to those formed by whole granules, with internal diameter averaging 160 Å (Fig. 2). In addition to circular lesions, incompletely polymerized material was also frequently observed (Fig. 2). The lesions resembled the polyperforin 1 lesions described previously for intact CTLL (IL-2-dependent CTL line) and NK clones (6, 7), indicating that the purified protein corresponded to the putative PFP/P1 monomer.

Planar Bilayer Measurements and Electrical Properties of PFP/P1. Planar bilayer membranes with high impedance were used to analyse the molecular sieving properties of PFP/P1. Exposure of bilayers to the purified protein at micromolar levels induced a rapid change in membrane conductance (Fig. 3*A*). Using lower amounts of protein this current change could be resolved as a progressive and irreversible incorporation of discrete current jumps (Fig. 3*C*). Current jumps were heterogenous in size, the minimal unit being identified as a 400 pS step in 0.1 M NaCl.

Symmetry of Current Response and Voltage Dependence. The current produced by this PFP/P1 was symmetrical respective to the polarity of the applied voltage (Fig. 3*B*). Little decay of the applied current was observed at transmembrane potentials below 100 mV, with most of the channels remaining open throughout the experiments. To study the voltage dependence of PFP/P1 channels, voltage pulses were applied to bilayers treated with PFP and the resultant current

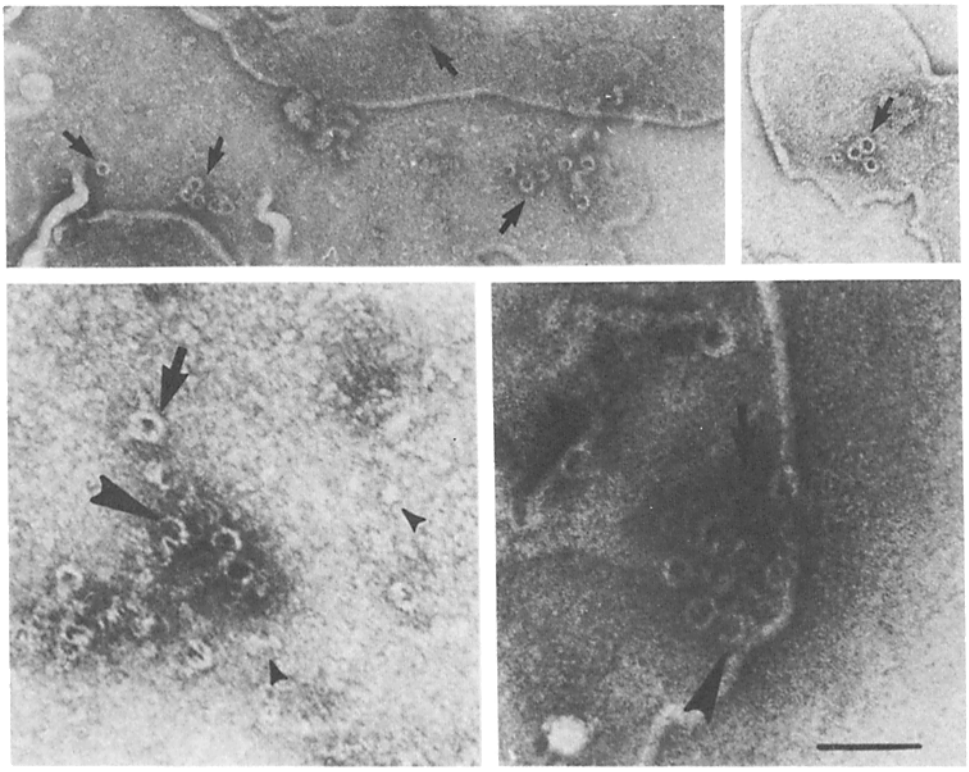

FIGURE 2. Membrane lesions on SRBC membranes produced by PFP/P1. The four panels show selected images of typical ring structures of 160 Å internal diameter (arrows) and some incompletely polymerized tubules (arrowheads). Scale bar: upper panels, 250 nm; lower panels, 85 nm.

responses were recorded (Fig. 3*D*). The current was allowed to relax at a given voltage pulse for 90 s, and the final steady-state current was used to generate current-voltage (I·V) plots. The I·V relationships obtained for PFP/P1 showed little deviation from linearity, that is, steady-state current obtained by applying increasing voltage pulses to a PFP-containing bilayer showed little relaxation with voltage pulses up to 110 mV (Fig. 3*D*). Only at voltages exceeding 110 mV, the current records became noisy, and channel closing was observed more frequently. The observation of this behavior was further substantiated by experiments in which continuous voltage ramps from −150 to +150 mV lasting 0.7–50 s were applied to PFP/P1-containing bilayers, and the corresponding currents were measured. Under these conditions, linear I·V plots were generated, with some current noise and nonlinearity occurring only at voltages >70 mV (not shown).

Requirement for Ca^{2+} in Membrane-binding and Channel Activity of PFP. Incorporation of PFP into the bilayer occurred spontaneously at room temperature (20–22°C), but only in the presence of Ca^{2+}. Lowering Ca^{2+} to micromolar levels using CaEGTA buffers (30) inhibited the formation of channels by PFP/P1 (not shown). Incorporation of soluble PFP/P1 into the bilayer was only observed at

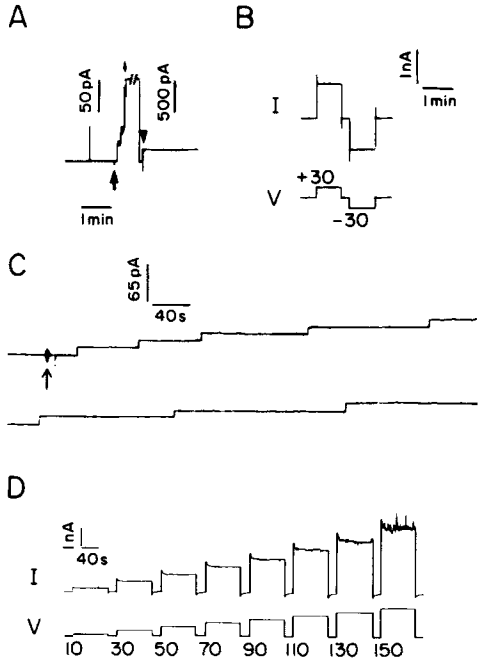

FIGURE 3. (*A*) Conductance increase in planar bilayer mediated by PFP/P1. The planar bilayer was formed in 0.1 M NaCl, 1 mM $CaCl_2$, 3 mM NaN_3, 10 mM Hepes, pH 7, and clamped at a constant +30 mV. PFP/P1 from CTLL-R8 was added into the *cis* side to 75 ng/ml (large arrow) followed by stirring for 15 s. Note the upward deflection of current until it went off-scale (small arrow). Current remained off-scale for 10 min (trace deleted) until the amplifier gain was turned down 10-fold (arrowhead), bringing current trace back. Note the smooth current trace without any channel fluctuations. (*B*) Symmetry of current response to voltages of opposite polarites. Bilayer prepared and treated with PFP/P1 (as in A) for 30 min before application of two voltage steps of 30 mV of opposite signs, as indicated. Lower part shows voltage tracing (V) and upper panel shows the current record (I). Note again the absence of any channel fluctuations following the capacitative transient. 22°C; resolution 2 ms. (*C*) Slow step-wise current increments associated with incorporation of lower amounts of PFP into lipid bilayer. The bilayer was prepared as in *A* and clamped at +35 mV. PFP was added to 12 ng/ml (arrow), followed by stirring (noise). (*D*) Steady-state current values at different voltages. The planar bilayer was prepared as in *A*. 40 min after treatment with 0.25 μg/ml PFP/P1, it was subjected to voltage increments (V) of similar duration, and rested at 0 mV between every two pulses. Note the increase of noise in the current record only at voltages higher than 110 mV.

Ca^{2+} levels over 50–100 μM. In the absence of Ca^{2+} (using buffers chelated with EGTA), PFP/P1 did not bind to bilayers, as perfusion of the chamber with fresh buffer followed by supplementation of 1 mM Ca^{2+} did not result in subsequent channel formation. Once channels were incorporated into the bilayer, depletion of Ca^{2+} from the membrane bathing solution had no effect on channel characteristics (not shown). Together, these observations suggest that Ca^{2+} triggers not only polymerization of PFP/P1, but also the attachment of this protein to target membranes. This effect could be due to certain conformation changes in PFP/P1 produced by Ca^{2+}, which might expose hydrophobic domains in PFP, allowing its subsequent interaction with lipids.

Single-Channel Fluctuations and Different Pore Sizes. Slow single-channel fluc-

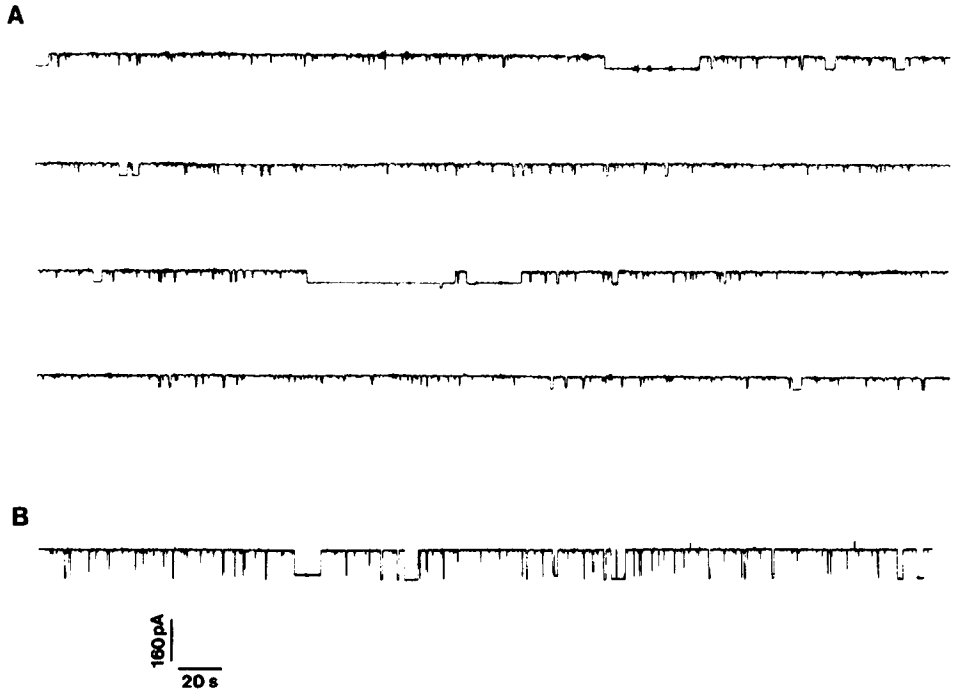

FIGURE 4. (*A*) Single-channel fluctuations associated with PFP/P1. The bilayer, prepared as in Fig. 3, was exposed to 0.5 ng/ml of purified PFP from CTLL-A2. The trace shows a continuous recording from upper left to lower right, obtained 10 min after addition of protein, with bilayer clamped at +120 mV. The upward deflections represent channel openings. Note the slow channel fluctuations of 400 pS observed at this voltage. Resolution, 1 ms. (*B*) PFP/P1 was reconstituted into lipid vesicles and incorporated into planar bilayer. Proteoliposomes (2 μg PFP/P1) were fused with bilayer as described in Materials and Methods. The current trace was obtained 15 min after perfusion of bilayer chamber with urea-free buffer. Note the 1 nS channel step.

tuations were observed infrequently at low transmembrane potentials. As noted, even at potentials exceeding 100 mV, most of the channels dwelled in the open state, with infrequent closings of relatively short durations. Single channel events associated with low amounts of PFP/P1 in the bilayer were similar for the PFPs extracted from all cell lines (Fig. 4).

Purified PFP polymerized in lipid vesicles at 37°C and incorporated into planar bilayers by a fusion protocol (see Materials and Methods) resulted in channels of larger unit conductances (unit of 1–6 nS in 0.1 M NaCl) when compared with PFP/P1 incorporated spontaneously into bilayers (400 pS) (Fig. 4*B*). This could be attributed to formation of complete tubules (consequently with larger unit conductances) in lipid vesicles as opposed to the smaller channels formed directly in the planar bilayer by soluble PFP.

Ion Selectivity. The ion selectivity of the channels was calculated from the reversal potential ($\mathscr{E}_r$) required to null the current due to a 10-fold higher salt gradient across the bilayer, with higher concentration on the *cis* side; selectivity was then obtained by means of the Nernst-Planck equation. The $\mathscr{E}_r$ obtained from many-channel-containing bilayers bathed in similar salt solutions varied in

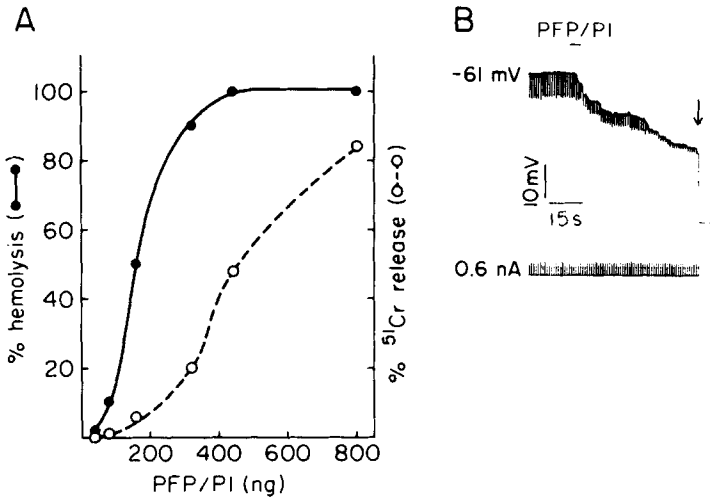

FIGURE 5. (*A*) Cytolysis produced by purified PFP/P1. Lysis of SRBC and E14 cells was assayed as described in Materials and Methods. The amount of protein refers to total protein per 100 μl assay. The PFP/P1 used was that obtained from CTLL-All using the Mono Q column. Lysis was observed in the absence of Ca^{2+}. (*B*) PFP/P1 rapidly depolarized the resting potential of cultured chicken myocytes. Note the rapid depolarization, associated with an increase in membrane conductance, after addition of protein. The arrow indicates withdrawal of microelectrode from cell.

different experiments. This result could be due to channels having marked differences in sizes, since the $\mathscr{E}_r$s of single channels varied accordingly with their unit sizes, the larger units showing lower $\mathscr{E}_r$s. For instance, for a 10-fold transmembrane gradient of KCl, the $\mathscr{E}_r$ ranged from +2 to −4 mV. $\mathscr{E}_r$ for NaCl ranged from +7 to −13 mV and for $CaCl_2$, +15 to +22 mV. Biionic experiments with 0.2 M KCl in *cis* challenged with 0.2 M NaCl (*trans*) produced a $\mathscr{E}_r$ of −4 to −8 mV. PFP/P1 channels were also permeable to Li^+, Mg^{2+}, Zn^{2+}, and $EGTA^{2-}$. The magnitude of the current driven through each channel increased proportionally with an increase in the ionic strength of the membrane bathing solution (tested with KCl and NaCl). Thus, it can be inferred that PFP/P1 channels behave as large, ion nonselective, aqueous pathways through the bilayer.

Cytolytic Activity of the Purified PFP/P1. In addition to potent hemolytic activity, PFP/P1 lysed T cell lymphoma E14 cells (Fig. 5*A*). Other cell lines susceptible to lysis by PFP/P1 include J774.2, S49.1, K562, S194, YAC-1, and 3T3 cells (data not shown). No cell specificity was observed, although cell lines varied in their susceptibility to lysis. Myoblasts treated with PFP/P1 showed immediate membrane depolarization (Fig. 5*B*), indicating that PFP/P1 must have functionally assembled into pores in the target membrane. Using $[^3H]Ph_4P^+$ as the voltage-sensitive probe, J774.2 and P814 cells also showed rapid membrane depolarization following exposure to PFP/P1 (not shown). In all experiments, the dose required to induce membrane depolarization was several-fold lower than that required to achieve cell lysis.

Discussion

The 70–75 kD PFP/P1 from H2-restricted T cell granules was extracted to apparent homogeneity and was shown to be largely responsible for the membrane lesions inflicted by whole effector T cells. PFP/P1 channels showed certain electrical properties that would be expected for large and stable transmembrane tubules. We have also obtained some preliminary information using whole cell patch-clamp recordings of cultured cells exposed to PFP/P1 that also suggest functional membrane damage by this protein (15). Moreover, purified PFP/P1 depolarized the membrane of cultured cells (Fig. 5*B*), indicating that the surface effect produced by PFP/P1 must not be restricted to model lipid membranes. The tumor cytolytic activity associated with the purified PFP/P1 (Fig. 5*A*) shows that the purified protein may bypass the need for intact cells or granules. It is possible that the release of PFP/P1 into restricted intercellular spaces between the effector and target cells may have a concentration effect, raising its local concentration many-fold. Recent results from our laboratory indicate that PFP/P1 is a secretory protein (31). Ca^{2+} appears to be required for the cellular release of the pore-former (31). Ca^{2+} is therefore thought to be required for both the fusion of granules with plasma membranes (i.e., degranulation) and the assembly of PFP/P1 into tubular lesions.

The Ca^{2+}-dependent binding of the purified protein to membranes and polymerization into macromolecular tubular complexes may be due to conformation change with the exposure of a hydrophobic domain in this molecule. Ca^{2+} appears to be required for the formation of stable, large ion channels. The absence of Ca^{2+} results in the formation of smaller channels by PFP/P1 with rapid flickering activity.

It is intriguing that PFP/P1 that had been polymerized in lipid vesicles before transfer to planar bilayers is associated with channels of larger size when compared with those produced by direct exposure of planar bilayers to soluble protein. This observation was similar to that made earlier with granule-derived material that had been incubated extensively at 37°C before reconstitution into planar bilayers. Such material showed larger single channel steps (1–6 nS in 0.1 M NaCl) than channels formed by granule proteins added directly to lipid bilayers (13). By modeling PFP/P1 channels as transmembrane tubules, this high unit conductance (1–6 nS) would correspond to a minimal functional diameter at 60 Å.

The smaller size of the channels observed here with soluble PFP/P1 could be attributed to polymerization of PFP into incomplete rings (frequently observed under electron microscopy), with formation of functional pores of smaller size. Formation of incomplete rings in planar bilayers after direct exposure of bilayers to soluble PFP/P1 would be favored, since all planar bilayer experiments described here were performed at 22–24°C, which would normally result in the formation of incomplete tubules, as evidenced by ultrastructural analysis. Thus, it is possible that PFP/P1 may produce effective membrane damage without undergoing complete polymerization to form the circular lesions visible by electron microscopy. Additional experiments are needed to substantiate this intriguing possibility.

Stable transmembrane pores produced and secreted by cytotoxic T cells could play an active role in cell killing by inserting into target membranes, disrupting the target cell transmembrane electrochemical gradient, and allowing ions and macromolecules to equilibrate across the plasma membranes. Alternatively, the formation of a transmembrane conduit of the size described here could allow the membrane passage of other toxic effector molecules (nucleases, proteases) into the target cells. A closely-related PFP/P1 was also recently purified from cloned murine lymphocytes that displayed high NK activity and that presented no histocompatibility restrictions (18); it was also purified from human NK cell clones (unpublished observations). The PFP/P1 extracted from these NK-like cells also has a M_r of 70–75 kD as analyzed by SDS-PAGE, and forms large voltage-resistant channels in planar bilayers (18, unpublished observations). Other immune cells that produce PFPs include eosinophils (32). Pore-forming activity has been described for a number of bacterial toxins and antibiotics (33, 34). A PFP/P1 from *Entamoeba histolytica* (22, 35, 36), which may be responsible for the contact-dependent cytolysis mediated by that protozoan, has also been extracted. It is interesting that the 70–75 kD protein described here bears close structural and functional homology to the ninth component of complement (C9); C9 polymerizes spontaneously at 37°C to form structural and functional transmembrane tubules similar to the ones described here; moreover, C9 and PFP/P1 show immunological crossreactivity (Young, J., Z. Cohn, and E. Podack, manuscript submitted for publication). Thus, the T lymphocyte PFP/P1 may represent one member of a wide group of proteins that may have evolutionally conserved the pore-forming activity as an effective means of inflicting damage to target membranes.

Summary

Histocompatibility-restricted cytotoxic T lymphocytes produce circular lesions on target cell membranes. The pore-forming protein (PFP or perforin 1) that forms these membrane lesions has been purified from lymphocytes. At 37°C, in the presence of Ca^{2+}, this protein polymerizes into a supramolecular tubular complex of $M_r > 10^6$ that partially resists dissociation by SDS and reducing agents. It incorporates spontaneously into planar lipid bilayers during polymerization to form nonselective ion channels, showing heterogeneous size distribution, the smallest conductance per unit being identified as 400 pS in 0.1 M NaCl. PFP/P1 that had been assembled in lipid vesicles before incorporation into planar bilayer show much larger single channel conductance, ranging from 1 to 6 nS in 0.1 M NaCl, suggesting that PFP/P1 may assume multiple functional sizes in proportion to its state of polymerization. The reconstituted channels are relatively voltage-insensitive, with most channels persisting in the open state for seconds to minutes. Nucleated cells are rapidly depolarized by this protein. The purified protein lyses a variety of tumor cells. Polymerization and functional channel activity are absolutely Ca^{2+}-dependent. The activity of this protein may play a direct role in T lymphocyte–mediated cytolysis.

We thank S. S. Ko and M. A. DiNome for their excellent technical assistance. Discussions

with and assistance throughout this work from Dr. C. F. Nathan and M. A. Palladino were most helpful.

Received for publication 12 March 1986.

References

1. Berke, G. 1983. Cytotoxic T lymphocytes. How do they function? *Immunol. Rev.* 72:5.
2. Trinchieri, G., and B. Perussia. 1984. Human natural killer cells: biologic and pathologic aspects. *Lab. Invest.* 50:489.
3. Herberman, R. B. 1982. Natural killer cells and their possible relevance to transplantation biology. *Transplantation.* 34:1.
4. Podack, E. R. 1985. Molecular mechanism of lymphocyte-mediated tumor lysis. *Immunol. Today.* 6:21.
5. Dourmashkin, R. R., P. Deteix, C. B. Simone, and P. A. Henkart. 1980. Electron microscopic demonstration of lesions on target cell membranes associated with antibody-dependent cellular cytotoxicity. *Clin. Exp. Immunol.* 43:554.
6. Podack, E. R., and G. Dennert. 1983. Cell-mediated cytolysis: assembly of two types of tubules with putative cytolytic function by cloned natural killer cells. *Nature (Lond.).* 302:442.
7. Dennert, G., and E. R. Podack. 1983. Cytolysis by H-2-specific T killer cells. Assembly of tubular complexes during the lytic reaction. *J. Exp. Med.* 157:1483.
8. Henkart, P. A., P. J. Millard, C. W. Reynolds, and M. P. Henkart. 1984. Cytolytic activity of purified cytoplasmic granules from cytotoxic rat large granular lymphocyte tumors. *J. Exp. Med.* 160:75.
9. Podack, E. R., and P. J. Konigsberg. 1984. Cytolytic T cell granules. Isolation, structural, biochemical, and functional characterization. *J. Exp. Med.* 160:695.
10. Millard, P. J., M. P. Henkart, C. W. Reynolds, and P. A. Henkart. 1984. Purification and properties of cytoplasmic granules from cytotoxic rat LGL tumors. *J. Immunol.* 132:3197.
11. Blumenthal, R., P. J. Millard, M. P. Henkart, C. W. Reynolds, and P. A. Henkart. 1984. Liposomes as targets for granule cytolysin from cytotoxic large granular lymphocyte tumors. *Proc. Natl. Acad. Sci. USA.* 81:5551.
12. Young, J. D.-E, C. F. Nathan, and Z. A. Cohn. 1985. Interaction of immune cells with target cell membranes: is there a common mechanism of killing? *J. Cell. Biochem.* 9(Suppl.):161.
13. Young, J. D. -E., C. F. Náthan, E. R. Podack, M. A. Palladino, and Z. A. Cohn. 1986. Functional channel formation associated with cytotoxic T cell granules. *Proc. Natl. Acad. Sci. USA.* 83:150.
14. Masson, D., and J. Tschopp. 1985. Isolation of a lytic, pore-forming protein (perforin) from cytolytic T-lymphocytes. *J. Biol. Chem.* 260:9069.
15. Podack, E. R., J. D. -E. Young, and Z. A. Cohn. 1985. Isolation and biochemical and functional characterization of perforin 1 from cytolytic T cell granules. *Proc. Natl. Acad. Sci. USA.* 82:8629.
16. Nathan, C. F., J. A. Mercer-Smith, N. M. DeSantis, and M. A. Palladino. 1982. Role of oxygen in T cell-mediated cytolysis. *J. Immunol.* 129:2164.
17. Borregard, N., J. M. Heiple, E. R. Simons, and R. A. Clark. 1983. Subcellular localization of the *b*-cytochrome component of the human neutrophil microbicidal oxidase: translocation during activation. *J. Cell Biol.* 97:52.
18. Young, J. D.-E, H. Hengartner, E. R. Podack, and Z. A. Cohn. 1986. Purification

and characterization of a cytolytic pore-forming protein from granules of cloned lymphocytes with natural killer activity. *Cell.* 44:849.

19. Young, J. D.-E, L. G. Leong, M. A. DiNome, and Z. A. Cohn. 1986. A semi-automated hemolysis microassay for membrane lytic proteins. *Anal. Biochem.* 154:649.
20. Young, J. D.-E, M. Blake, A. Mauro, and Z. A. Cohn. 1983. Properties of the major outer membrane protein from *Neisseria gonorrhoeae* incorporated into model lipid membranes. *Proc. Natl. Acad. Sci. USA.* 80:3831.
21. Kagawa, Y., and E. Racker. 1971. Partial resolution of the enzymes catalysing oxidative phosphorylation. Reconstitution of vesicles catalysing ^{32}Pi-adenosine triphosphate exchange. *J. Biol. Chem.* 246:5477.
22. Young, J. D.-E, T. M. Young, L. P. Lu, J. C. Unkeless, and Z. A. Cohn. 1982. Characterization of a membrane pore-forming protein from *Entamoeba histolytica. J. Exp. Med.* 156:1677.
23. Young, J. D.-E, J. C. Unkeless, T. M. Young, A. Mauro, and Z. A. Cohn. 1983. Role for mouse macrophage IgG Fc receptor as ligand-dependent ion channel. *Nature (Lond.).* 306:186.
24. Montal, M., and P. Mueller. 1972. Formation of bimolecular membranes from lipid monolayers and a study of their electrical properties. *Proc. Natl. Acad. Sci. USA.* 69:3561.
25. Zimmerberg, J., F. S. Cohen, and A. Finkelstein. 1980. Fusion of phospholipid vesicles with planar phospholipid bilayer membranes. I. Discharge of vesicular contents across the planar membrane. *J. Gen. Physiol.* 75:241.
26. Young T. M., and J. D.-E Young. 1984. Protein-mediated intermembrane contact facilitates fusion of lipid vesicles with planar bilayers. *Biochim. Biophys. Acta.* 775:441.
27. Paterson, B., and J. Prives. 1973. Appearance of acetylcholine receptor in differentiating cultures of embryonic chick breast muscle. *J. Cell Biol.* 59:241.
28. Segal, M., and J. L. Barker. 1984. Rat hippocampal neurons in culture: properties of GABA-activated Cl^- ion conductance. *J. Neurophysiol.* 51:500.
29. Laemmli, U. K. 1970. Cleavage of structural proteins during the assembly of the head of bacteriophage T4. *Nature (Lond.).* 227:680.
30. Young, G. P. H., J. D.-E Young, A. K. Deshpande, M. Goldstein, S. S. Koide, and Z. A. Cohn. 1984. A Ca^{2+}-activated channel from *Xenopus laevis* oocyte membranes reconstituted into planar blayers. *Proc. Natl. Acad. Sci. USA.* 81:5155.
31. Young, J. D.-E, L. G. Leong, C.-C. Liu, A. Damiano, and Z. A. Cohn. 1986. Extracellular release of lymphocyte cytolytic pore-forming protein following ionophore stimulation. *Proc. Natl. Acad. Sci. USA.* In press.
32. Young, J. D.-E, C. G. B. Peterson, P. Venge, and Z. A. Cohn. 1986. Mechanism of membrane damage mediated by human eosinophil cationic protein. *Nature (Lond.).* In press.
33. Latorre R., and O. Alvarez. 1981. Voltage-dependent channels in planar bilayer membranes. *Physiol. Rev.* 61:77.
34. Schein, S. J., B. L. Kagan, and A. Finkelstein. 1978. Colicin K acts by forming voltage-dependent channels in phospholipid bilayer membranes. *Nature (Lond.).* 276:159.
35. Lynch, E. C., I. M. Rosenberg and C. Gitler. 1982. An ion-channel forming protein produced by *Entamoeba histolytica EMBO (Eur. Mol. Biol. Organ.) J.* 1:801.
36. Young, J. D.-E, and Z. A. Cohn. 1985. Molecular mechanisms of cytotoxicity mediated by *Entamoeba histolytica*: characterization of a pore-forming protein (PFP). *J. Cellular Biochem.* 29:299.